Supporting Information

Ghosh et al. 10.1073/pnas.1009193107

SI Materials and Methods

In Vitro T-Cell Differentiation. CD4 T cells were isolated and activated with 1 μg/mL hamster α-mouse CD3 (clone 145-2C11) (ATCC) and 1 μg/mL hamster α-mouse CD28 (BD Pharmingen) for T-cell differentiation under nonpolarizing conditions (Th0). In addition, 10 ng/mL of IL-12 and 10 μg/mL of αIL-4 were added for Th1 differentiation; 1,000 U/mL IL-4, 5 μg/mL of αIFNγ, and 3 μg/mL of αIL-12 were added for Th2 differentiation. $CD4CD25^+$ T cells were depleted from purified CD4 T cells using a CD25 microbead MACS kit (Miltenyi Biotech); ∼76–84% of CD4 $CD25^+$ double positive cells, in both WT and AVT mice, express Foxp3. For Th17 differentiation, $CD4CD25^-$ T cells were plated with 2 μg/mL α-mouse CD3 and 2 μg/mL α-mouse CD28; a cocktail of TGFβ (3 ng/mL), IL-6 (30 ng/mL), αIFNγ (10 μg/mL), and αIL-4 (10 μg/mL) was added for T-cell differentiation under Th17 conditions (1). For iTreg generation, TGFβ (3 ng/mL) was used in addition to αCD3+αCD28. CD8 T cells were isolated using the Dynal CD8 T cell-negative isolation kit (Invitrogen) and activated with 1 μg/mL α-mouse CD3 and 1 μg/mL hamster anti-mouse CD28.

T-Cell Activation and Flow Cytometry. T cells were collected from in vitro cultures at indicated time points, washed, counted, and stimulated for 4–5 h with 20 nM phorbol myristate acetate (PMA) and graded concentrations of ionomycin; where indicated, CsA was added at a final concentration of 2 μM 20 min before activation. Brefeldin A was added at 10 μg/mL for the final 2–2.5 h of stimulation. T cells were stained for surface markers, fixed with 4% paraformaldehyde, and then permeabilized in saponin buffer and stained for intracellular cytokines. For Foxp3 staining, a separate Foxp3 staining kit (eBioscience) was used as per the manufacturer's instructions. Foxp3 expression was measured 48–72 h after activation. Data were collected using FACSCalibur or FACSCanto II flow cytometers (BD Pharmingen).

ChIP. T cells differentiated under Th17 conditions in vitro, as described above, were expanded for 6–7 d using 15 ng/mL recombinant IL-23 (R&D systems). Th17 cells were activated using 20 nM PMA and 1 μM ionomycin for ∼30 min. Cells were fixed in 1% formaldehyde for 30 min followed by addition of 125 mM glycine. Cells were spun, washed in cold PBS, and sonicated in lysis buffer containing protease inhibitors. Supernatants collected by spinning sonicated lysates at maximum speed were precleared with protein A beads. Chromatin immunoprecipitation was performed using rabbit polyclonal αNFAT1 (67.1) or polyclonal rabbit antiserum (as control), followed by addition of protein A beads. Beads were washed, treated with RNase A, and Proteinase K. After cross-link reversal by incubation at 65 °C, DNA was isolated from the mixture using QIAquick spin columns (Qiagen) and used as a template for real-time PCR. Primers used for ChIP PCRs have been described elsewhere (2, 3).

1. Bettelli E, et al. (2006) Reciprocal developmental pathways for the generation of pathogenic effector TH17 and regulatory T cells. *Nature* 441:235–238.
2. Akimzhanov AM, et al. (2007) Chromatin remodeling of interleukin-17 (IL-17)-IL-17F cytokine gene locus during inflammatory helper T cell differentiation. *J Biol Chem* 282: 5969–5972.
3. Lee CG, et al. (2009) A distal cis-regulatory element, CNS-9, controls NFAT1 and IRF4-mediated IL-10 gene activation in T helper cells. *Mol Immunol* 46:613–621.

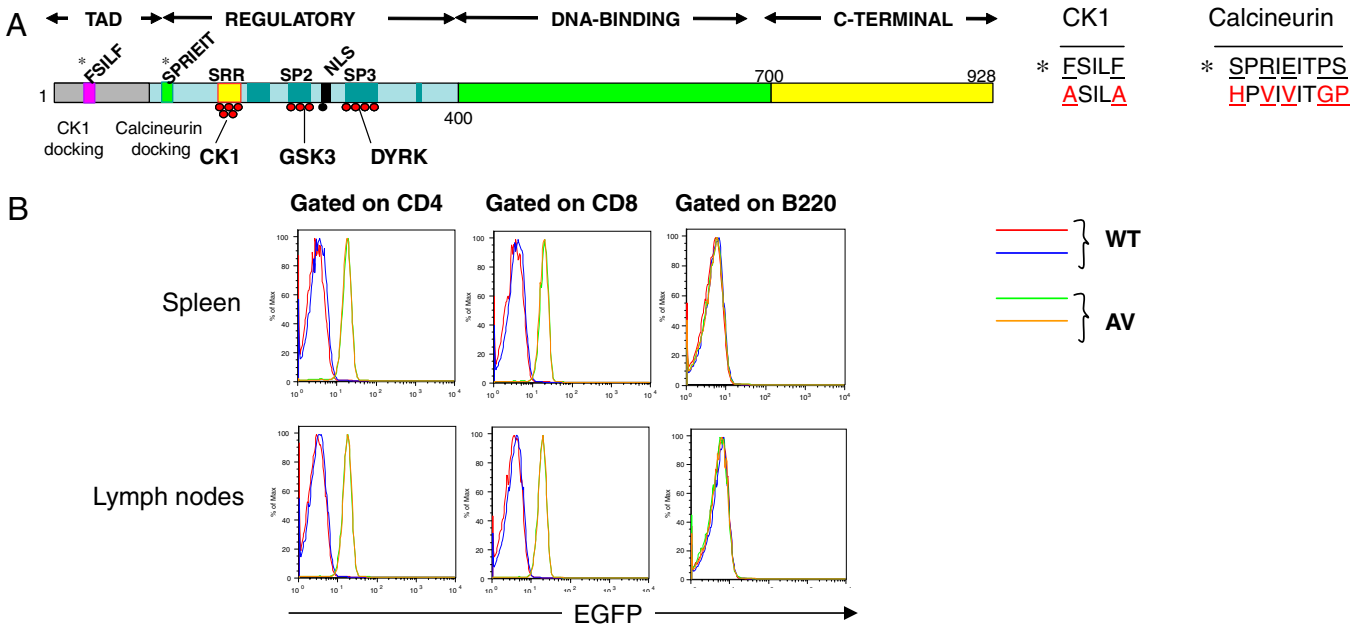

Fig. S1. (*A*) Schematic diagram of NFAT1, depicting the transactivation (TAD), regulatory and DNA-binding domains; NLS, nuclear localization signal. Red circles indicate conserved serine residues which are reversibly phosphorylated by CK1 (SRR motif), GSK3 (SP2 motif) and DYRK (SP3 motif) (1). (*B*) EGFP expression in AVT mice; transgene expression was monitored through the expression of EGFP via an internal ribosome entry site (IRES) (1).

1. Muller MR, et al. (2009) Requirement for balanced Ca/NFAT signaling in hematopoietic and embryonic development. *Proc Natl Acad Sci USA* 106:7034–7039.

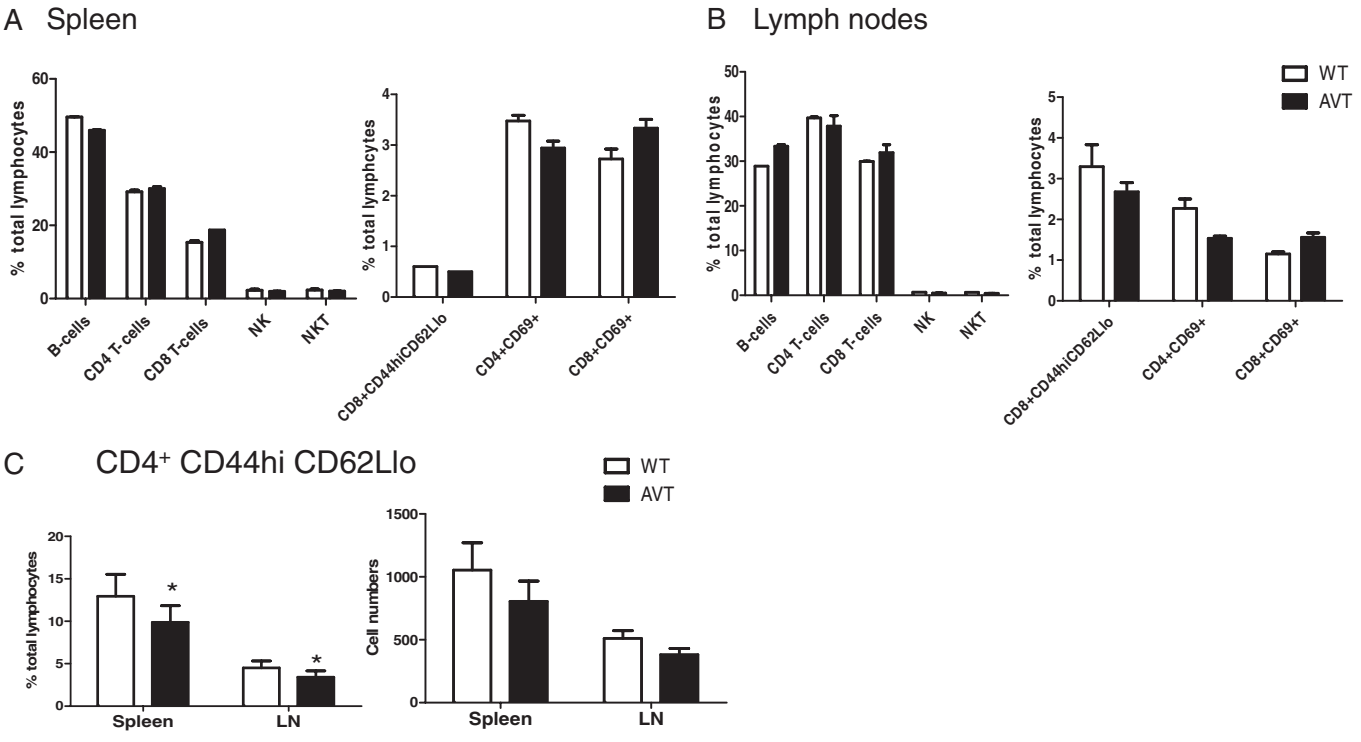

Fig. S2. (*A* and *B*) No appreciable difference between AVT and WT mice in most lymphoid compartments examined; age = 6 wk; $n = 2$. (*C*) Decreased frequency of CD4 CD44hiCD62Llo effector/activated T cells in spleen and lymph nodes of AVT mice, relative to WT; age = 6 wk, $n = 4$ per group; $^*P < 0.05$ by Student's *t* test.

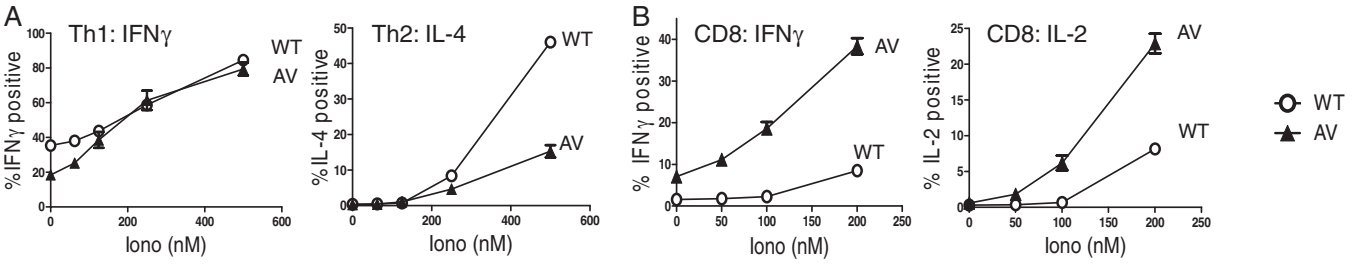

Fig. S3. (*A*) CD4 T cells from AVT and WT mice were differentiated under Th1 or Th2 conditions. Cells were allowed to rest and restimulated on day 5 with 20 nM PMA and the indicated concentrations of ionomycin. (*B*) CD8 T cells from WT and AVT mice were activated with plate-bound αCD3/αCD28 for 48 h and restimulated as in *A*.

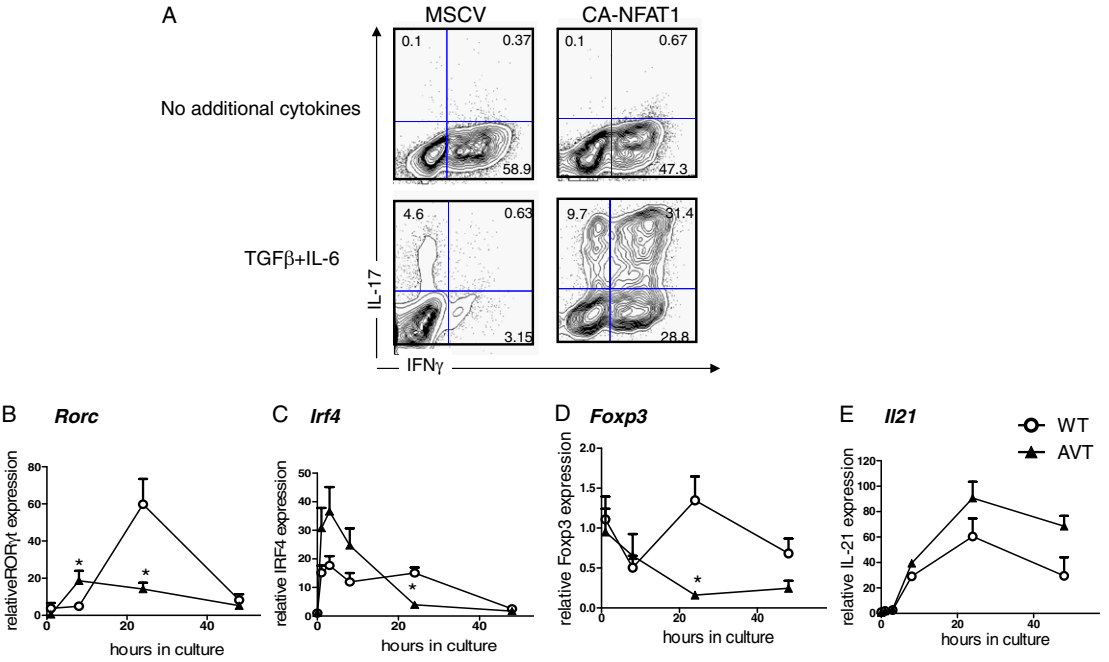

Fig. S4. (*A*) Purified CD4 T cells from C57BL/6 mice were activated using αCD3+αCD28 and transfected with CA-NFAT1 or vector alone, either in the absence or presence of 3 ng/mL TGFβ and 30 ng/mL IL-6; this was followed by intracellular staining for IFNγ and IL-17 and FACS. Naïve CD4 T cells from WT, NFAT1$^{-/-}$ and AVT NFAT1$^{-/-}$ mice were cultured for the indicated time periods under Th17-polarizing conditions (*B*–*E*), followed by isolation of total RNA; mRNA expression was quantified by real-time RT-PCR (*SI Materials and Methods*). ROR, retinoic acid receptor related orphan receptor; IRF, Interferon regulatory factor. Data are representative of at least two independent experiments.

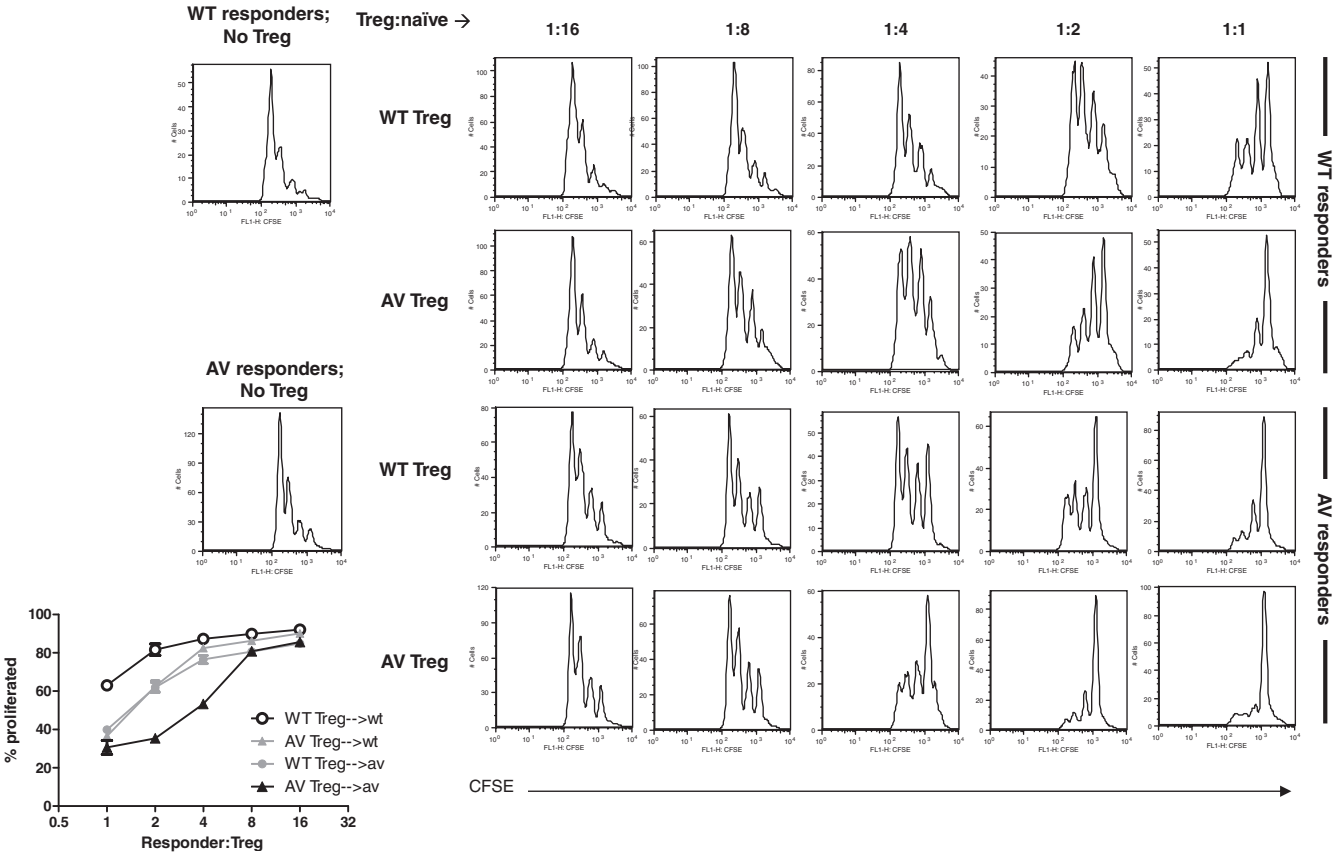

Fig. S5. Increased suppressive effects of AV Tregs on WT or AV responders, compared with WT Tregs, and lower baseline proliferation of AV responders compared with WT; all cells isolated from 10-wk-old WT or AVT mice. (*Bottom Left)* Graphical representation of FACS data; % proliferated indicates the percentage of total cells having undergone one or more divisions, as measured by carboxyfluorescein succinimidyl ester (CFSE) dilution. In vitro proliferation assays performed as described in *Materials and Methods*. Naïve AVT responder cells were observed to be modestly less proliferative compared to their WT counterparts.

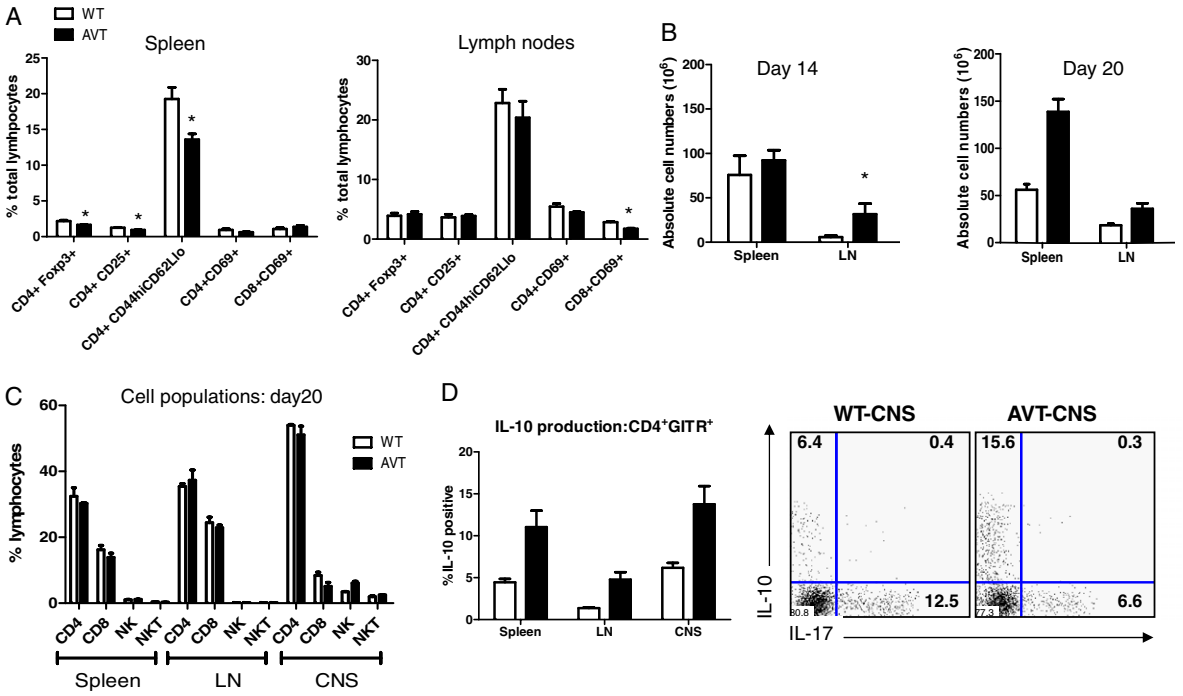

Fig. S6. (*A*) Lymphocyte populations in WT and AVT mice at day 6 following MOG immunization. (*B*) Absolute numbers of lymphocytes in spleen and lymph nodes of AVT and WT mice at days 14 and 20 following MOG immunization; data from two independent experiments; $*P < 0.05$ by Student's *t* test. (*C*) Lymphocyte subsets in spleen, lymph nodes, and CNS of WT and AVT mice at day 20 after MOG immunization. (*D*) Production of IL-10 and IL-17 in $CD4^+GITR^+$ cells from WT and AVT mice at day 20 after MOG immunization in spleens, lymph nodes, and CNS. (*Right*) Representative flow cytometry depicting IL-10/IL-17 production by $CD4^+GITR^+$ cells in the CNS of WT and AVT mice. Note that glucocorticoid-induced TNFR-related protein (GITR) is a surface marker for Tregs and also upregulated on T cells upon activation.

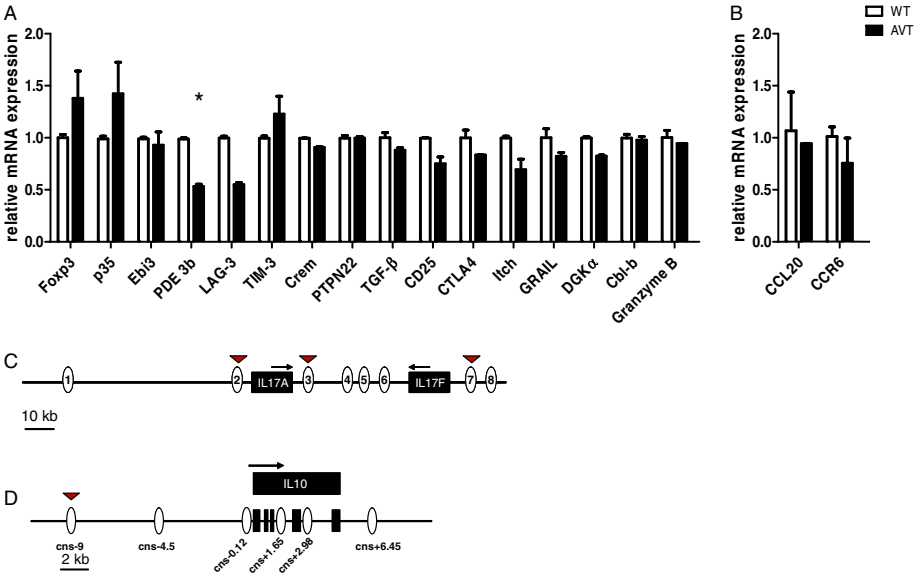

Fig. S7. (*A*) Expression of anergy/Treg associated genes (1–3) and (*B*) CCR6 and CCL20 in CD4 T cells purified from lymphocytes that were isolated from the CNS of WT and AVT mice during established EAE (day 25). (*C*) Schematic representation of the *Il17a-f* locus adapted from Akimzhanov et al. (4). Red triangles indicate the *CNS* regions bound by NFAT1. (*D*) Schematic representation of the *Il10* locus adapted from Lee et al. (5).

1. Shevach EM (2009) Mechanisms of foxp3+ T regulatory cell-mediated suppression. *Immunity* 30:636–645.
2. Borde M, et al. (2006) Transcriptional basis of lymphocyte tolerance. *Immunol Rev* 210:105–119.
3. Heissmeyer V, et al. (2004) Calcineurin imposes T cell unresponsiveness through targeted proteolysis of signaling proteins. *Nat Immunol* 5:255–265.
4. Akimzhanov AM, Yang XO, Dong C (2007) Chromatin remodeling of interleukin-17 (IL-17)-IL-17F cytokine gene locus during inflammatory helper T cell differentiation. *J Biol Chem* 282: 5969–5972.
5. Lee CG, et al. (2009) A distal cis-regulatory element, CNS-9, controls NFAT1 and IRF4-mediated IL-10 gene activation in T helper cells. *Mol Immunol* 46:613–621.

A

CNCS1	GCTGCTGTTTCCTTGAGAGGATTCTGACAGGAAGCCATAGAAATGCAAGCCAACACTGCCAGCTCTGGAAATAAAATAAATAATGACCCAGGTTCTATGCTCCTCAATGGGGGCAGAAGCCTGCGGGGCAAGAAAACCACAGAGGAGGAGGGACCTGCCTGCAACTTGTCCCCAGGTATGTCACTGAGCTGATTCTGCATGCTGCTGTCTCCTCTCTTTGTCCCCTGGCTGTTCCTGCCTTATCCAGC
CNCS2a	CAGCGTGTGGTTTGGTTTACTTATTTAATTTTAGACGATACTTTTCAGTGACATCCGTTTAGACTTGAAACCCAGTCAGTTGCTGACCTTGATTCTAAGGGTATCAGATGAAGTCAGCATTACCCAAGTGGGGGCCATCAGTCAAAGAATTTGCATGCGCCTCCTAACACATAGGTACTTGATTCTAAATGTACTTGGTTGGAAAAAAAAAATGGAAAGTTTTCTGACCCACTTTAAATCAATTTTTCAGTAAAAGACCAGTGAGGAACCCACCTAG
CNCS2b	CAGCCCTGGTCCTTAAACTGTAGCTGCCCAGTCTTGTAGCTGCTGTTTTGAATCTGCAGAGAAGCAAGATGGATACACTTGAAGGCCACTCCTGAGCAAAATCATCATTCCTAACCTACTGCTTTTGTTTATTCATTGCTATTTTCCTTCTGCAAAAAGTCAACCACAATGAACAGGTGAGACAAAACCTCATTTTATAAAACAGAAGAGCATGTCTACAAAAAAGATGAAGTAGGTCTCAGAAAGGCAAAGGCACAACGAAAGTGA
CNCS3	TTAGTGAGGTCGGGGAAGTGGACATGTCTGTGGTTAAAAGCAAAGAGGCTTAAAAGAGCTCAGATCAAAGGGGGCTTGTCCCTCACATACCTCATGCTGAATTACCACAGGTAGGTTACTTTCAGAAGTTCCTGGAAAGAGTTAGTCACTGCACTTTGCTCATGCCCATATGTCTGCCTGATATGAATGTGCTGCCATCAAA
CNCS4	TCGCCTCTTGACAAACAGTGTGGTTAACCAAGCTGTCTGCAGCCTTCCTGGTGAATCAGTAGCTCACAGTAGTGAGACTCGCCACAATAATATAACTCTGCTCTTGAGTCCAGAGAGAAATCAACGAGAAGCTCAAATCCGTGTGCCTTCTGTTACTGCAGTGAGGAAGATGTTTCCAATGAGGAAATCACAGGGACGAA
CNCS5	AGGCCCACAATGTAGGTCAGTCATCTTGGTTTACATTTGTGGAAGGAGAGCTCTGCAAACAGCCGCTTCCTTCCCCTGAGGTTACTGTAAGAAGTGGCCTACTTCAGGCAGATGGTGAGAAGCCAGCGTCGGGTCCCAGAATGCTTCTCATCGGCTCCCACACAGAGCATGCCGCACTCAAACTGAAACAGCTTCGGTACTGCCGCCTTTCAGAACCTACCACATGGGTGAGTCAGAGAGACTTCCCAGCCTG
CNCS6	TGCCTAGGGCTTGAGTGTCTTTAAAATACTAAGCACTTCATGCGACCGTGGCATCCCCTTCTAGGGGACAGCCACATTGAGGATGGACTTTATAGCACACAGAAGTGTCCAGGGTGGCCTTCCCATCATGGCTGCTTTTTCCATGGGGTTGGGTTTCAGAGCAACCAGCTGAGTGGCATACTTAACATACCAAAGCGGACCTG
CNCS7	CTGAGTTGGGGGCTGTGTATCCTGGAAGCTATAGCCTGCAGCCCTGCACAACCACGTTGCAGGTCCCAGGCAGACTTTCACTTACTCAGCTGCAGCCTGATTTCCTGCACTAAGCTGGATGGAATTAGTCAGCACACTACCCAGCCACCACGTCTGGGGAAAGCCCTGCTCACTGTCTGCTAATGTAAAGTCCGACACCCTCGATATG
CNCS8	CAGCAGACACACATGCAAGAGGGCCTAGGTTGACCTTTCTATTGCGAGGTTAAATGGTGGCCCTTAAAGCAGGAAGGCTTGGCTTTACTACAAGACACCTGAGGGGGCAGCTGTTCTCAGAACGGTACAGCTAAGCAGAGGCTAATATCCTCCTACAGGCTGTGGGGGAACGTTCAGGACTTAATAGTAAAAATATTCAGGGAAAACTTTAGATTCTTAATTCCCTCCCCTGAGG

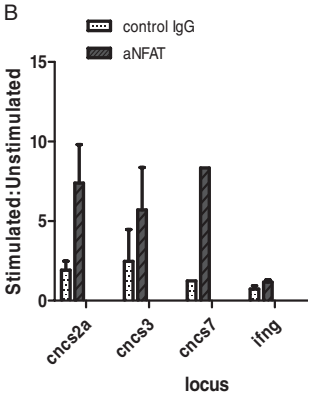

Fig. S8. (*A*) Sequence of CNCS regions in the *Il17-Il17f* locus (2); NFAT consensus sites corresponding to either strand have been underlined. (*B*) NFAT1 binds CNCS2a, 3 and 7 within the *Il17-Il17f* locus in CD4 T cells isolated from AVT mice and polarized under Th17-inducing conditions.

Table S1. Summary of incidence, day of onset of symptoms, mean clinical scores, and mortality of WT and AVT mice after EAE induction

Group	Incidence	Mean onset (d)	Mean maximum score	Mean score day 14	Mean score day 20	Mortality
WT (n = 33)	32 of 33	9.25 ± 0.96	4.25 ± 0.96	1.82 ± 1.01	2.9 ± 1.35	3 of 32 (9%)
AVT (n = 34)	33 of 34	9.5 ± 1	3.5 ± 0.5	1.62 ± 0.95	1.43 ± 0.9 ***	0 of 33 (0%)

Mean ± SD across four independent experiments.
*** $P < 0.0001$ by Student's t test.

Table S2. Primer sequences used for real-time RT-PCRs

Primer name	Sequence
Rorc	5-CGCTGA GAG GGCTTC AC-3
	5-GCA GGA GTA GGC CAC ATT ACA-3
Irf4	5-TCC GAC AGT GGT TGA TCG AC-3
	5-CCT CAC GAT TGT AGT CCT GCT T-3
Foxp3	5-ACT CGC ATG TTC GCCTACTTC AGA-3
	5-TGG CTC CTC TTC TTG CGA AACTCA-3
Il21	5-ATG GAG AGG ACC CTT GTC TGT C-3
	5-CTA GGA GAG ATG CTG ATG AAT C-3
Il17	5-ATC CAC CTC ACA CGA GGC ACA A-3
	5-AGATGA AGCTCT CCCTGG ACT CAT-3
Il17f	5-GCA CCC GTG AAA CAG CCA TGG TC-3
	5-GGC CGC TTG GTG GAC AAT GGG C-3
Ifng	5-GAG CCA GAT TAT CTC TTT CTA CC-3
	5-GTT GTT GAC CTC AAA CTT GG-3
Il10	5-ATA ACT GCA CCC ACT TCC CA-3
	5-TCA TTT CCG ATA AGG CTT GG-3
Il2	5-CTG CGG CAT GTT CTG GAT TTG ACT-3
	5-AGT CCA CCA CAGTTG CTG ACT CAT-3
Il22	5-CAT GCA GGA GGT GGT ACCTT-3
	5-CAG ACG CAA GCATTT CTC AG-3
IL-23Ra	5-CAG CGG CTT GAT TCT GAA GAG AGA-3
	5-ATG CAG CTG AAGTGT GAG GTG ACT-3